

Quasinormal modes of Kerr-like black bounce spacetime

Yi Yang,^{1,*} Dong Liu,^{2,†} Ali Övgün,^{3,‡} Zheng-Wen Long,^{4,§} and Zhaoyi Xu^{4,¶}

¹*School of Mathematics and Statistics,*

Guizhou University of Finance and Economics, Guiyang, 550025, China

²*Department of Physics, Guizhou Minzu University, Guiyang, 550025, China*

³*Physics Department, Eastern Mediterranean University,*

Famagusta, 99628 North Cyprus via Mersin 10, Turkey.

⁴*College of Physics, Guizhou University, Guiyang, 550025, China*

We investigate the quasinormal mode (QNM) spectrum of a Kerr-like black-bounce spacetime under massive scalar-field perturbations. Starting from the Kerr-like deformation of the Simpson–Visser black-bounce geometry, we derive the corresponding radial and angular equations and obtain the effective potential governing scalar perturbations. We show that the Kerr-like black-bounce spacetime inherits a characteristic double-peaked effective potential, analogous to the Schwarzschild-like black-bounce case, which is known to be associated with late-time echo signals. The QNM frequencies are computed by means of the Pöschl–Teller potential approximation and the semi-analytic WKB method (up to sixth order), and we demonstrate good agreement between these two approaches. We then analyze in detail how the QNM spectrum depends on the spin parameter a , the bounce parameter p that interpolates between black-hole and wormhole geometries, and the scalar-field mass μ . Our results indicate that increasing either a or p lowers both the real frequency and the magnitude of the imaginary part, leading to longer-lived modes. Moreover, the mass of the scalar field has a non-negligible impact on the ringdown spectrum. These features suggest that rotating black-bounce geometries may leave distinct imprints in the ringdown phase of gravitational-wave signals, and motivate future studies of echoes and parameter estimation in the context of present and upcoming detectors.

PACS numbers: 95.30.Sf, 04.70.-s, 97.60.Lf, 04.50.+h

Keywords: Modified gravity; Rotating black hole; Quasinormal modes; LIGO/Virgo; LISA; Superradiance; Black hole mimickers; gravitational wave astronomy .

I. INTRODUCTION

The first direct detections of gravitational waves (GWs) by the LIGO and Virgo Collaborations [1], together with the imaging of black-hole shadows by the Event Horizon Telescope (EHT) [2, 3], have opened a new era in strong-gravity physics. For the first time, highly dynamical, strong-field regimes of gravity — such as the merger and ringdown of compact binaries — can be probed observationally. This allows us to test general relativity (GR) and constrain alternative theories of gravity in regimes that were completely inaccessible only a decade ago [4–10].

Within this new observational window, the ringdown phase of a black-hole merger plays a particularly central role. After the highly non-linear merger, the remnant object relaxes to a stationary configuration by emitting damped oscillations — the quasinormal modes (QNMs). These modes are characterized by a discrete set of complex frequencies, whose real parts represent the oscillation frequencies while their imaginary parts encode the damping rates. In GR, the QNM spectrum of an astrophysical black hole is uniquely determined by its mass and spin, as dictated by the no-hair theorems. Measuring multiple QNMs thus provides a powerful test of the Kerr nature of the remnant and of the underlying theory of gravity [11–25].

At the same time, numerous extensions of GR and exotic compact-object models have been proposed in recent years. Alternative and modified gravity theories introduce additional degrees of freedom or new couplings, leading to field equations with different stationary solutions and distinct strong-field phenomenology [26–38]. Among the rich landscape of non-Kerr geometries, regular black holes and wormhole-like spacetimes are especially intriguing, as they resolve curvature singularities or interpolate between black holes and wormholes, while still providing observational signatures close to those of Kerr in appropriate limits. The QNM spectrum of such objects generically deviates from the Kerr case, offering a potential avenue for tests of the no-hair conjecture and of the underlying gravity theory [39–62].

* yiyang@mail.gufe.edu.cn

† dongliuvv@yeah.net

‡ ali.ovgun@emu.edu.tr

§ zwlong@gzu.edu.cn

¶ zyxu@gzu.edu.cn

A particularly elegant example of a regular spacetime is the black-bounce geometry introduced by Simpson and Visser [63]. By introducing a single parameter a into the Schwarzschild solution, they constructed a geometry that interpolates smoothly between a Schwarzschild black hole ($a = 0$ and $m \neq 0$) and a traversable wormhole ($a \geq 2m$). This idea has since been generalized in several directions, including new versions of the Schwarzschild-like black-bounce spacetime [64]. A broad range of physical properties of these spacetimes has been investigated: QNMs and possible gravitational-wave echoes [24, 65, 66], gravitational lensing in the weak and strong field regimes [67–69], absorption cross sections for scalar waves [70], and thin-shell wormhole constructions [71], among others. Rotating generalizations have also been studied: Mazza et al. constructed a rotating black-bounce model [72], whose QNMs were subsequently analyzed in [73], and charged black-bounce solutions were obtained in [74]. Using a Newman–Janis-type algorithm, Xu and Tang [75] constructed a Kerr-like black-bounce geometry, while Guerrero et al. explored its lensing and shadow properties [76]. Time evolution of perturbations and retrolensing signatures in related spacetimes have also been discussed in [77, 78].

In this context, Kerr-like black-bounce spacetimes provide a concrete and controlled framework in which to study continuous deviations from Kerr, including configurations that are regular or wormhole-like in the interior while remaining Kerr-like at large radii. From an observational point of view, the ringdown signal of a perturbed rotating black-bounce geometry may carry imprints of the underlying regular core or bounce structure, for example in the form of modified QNM spectra or late-time echoes associated with double-peaked effective potentials.

The main objective of this work is to characterize the QNMs of a Kerr-like black-bounce spacetime under massive scalar-field perturbations, and to quantify how deviations from the Kerr geometry — encoded in the bounce parameter p and in the choice of black-bounce profile — affect the ringdown spectrum. In particular, we aim to: derive the effective potential governing scalar perturbations in the Kerr-like black-bounce background constructed via the Newman–Janis algorithm; analyze the structure of this potential (including the appearance of double peaks) and its dependence on the rotation parameter a , the bounce parameter p , and the scalar-field mass μ ; compute the corresponding QNM frequencies using both the Pöschl–Teller potential approximation and the semi-analytic WKB method, and compare their accuracy; assess how the parameters (a, p, μ) shift the real and imaginary parts of the QNM spectrum, and discuss the implications for gravitational-wave ringdown observations and potential echo signatures.

In Sec. II we review the Kerr-like black-bounce spacetime, present the relevant metric functions, and derive the determinant and inverse metric components. In Sec. III we study massive scalar perturbations, derive the separated radial and angular equations, and obtain the effective potential in tortoise coordinates, illustrating its dependence on the key parameters. In Sec. IV we introduce the Pöschl–Teller potential approximation and the WKB method, compute the QNM spectrum, and compare the two approaches. We also analyze in detail how the QNM frequencies vary with a , p , and μ . Finally, in Sec. V we summarize our main results, discuss their physical implications, and outline possible directions for future work. Throughout the paper we adopt geometrized units with $G = c = 1$.

II. KERR-LIKE BLACK-BOUNCE SPACE-TIME

Regular spacetime metric is an interesting topic in current GR and black hole physics. It is a variant of Schwarzschild metric. In our research, we focus on black-bounce space-time which is a regular space-time that connects Schwarzschild black hole and wormhole. The Schwarzschild-like black-bounce space-time is generally read as [64]

$$ds^2 = -f(r)dt^2 + \frac{1}{g(r)}dr^2 + H(r) (d\theta^2 + \sin^2\theta d\phi^2), \quad (1)$$

where

$$\begin{aligned} f(r) &= g(r) = 1 - \frac{2Q(r)}{\sqrt{H(r)}}, \\ Q(r) &= \frac{M\sqrt{H(r)}r^k}{(r^{2n} + p^{2n})^{\frac{k+1}{2n}}}, \\ H(r) &= r^2 + p^2, \end{aligned} \quad (2)$$

where the non-negative parameter p can determine whether space-time is a black hole or a wormhole, M is the mass of compact object, n and k are natural number, that is, their values are $0, 1, 2, 3 \dots$. When $n = 1$ and $k = 0$, the black-bounce space-time degenerates to Simpson-Visser model [63]. Churilova et al. studied the quasinormal modes of this space-time, and found the echoes in the late stage [65]. In addition, we have studied another special case of Schwarzschild-like black-bounce space-time, and we also found the echoes in the late stage of quasinormal modes [79]. On the other hand, we obtained Kerr-like black-bounce space-time by using Newman-Janis algorithm [75]

$$ds^2 = - \left(1 - \frac{2M(r^2 + p^2)r^k}{(r^{2n} + p^{2n})^{\frac{k+1}{2n}} \Sigma} \right) dt^2 + \frac{\Sigma}{\Delta} dr^2 - \frac{4a \sin^2 \theta M(r^2 + p^2)r^k}{\Sigma (r^{2n} + p^{2n})^{\frac{k+1}{2n}}} dt d\varphi + \Sigma d\theta^2 + \frac{\sin^2 \theta}{\Sigma} \left((r^2 + p^2 + a^2)^2 - a^2 \Delta \sin^2 \theta \right) d\varphi^2, \quad (3)$$

where

$$\Delta = r^2 + a^2 + p^2 - \frac{2Mr^k(r^2 + p^2)}{(r^{2n} + p^{2n})^{\frac{k+1}{2n}}}, \quad \Sigma = r^2 + p^2 + a^2 \cos^2 \theta. \quad (4)$$

For $n = 1, k = 0, a = 0$, the rotating black bounce spacetime degenerates to Schwarzschild-like black bounce spacetime [63]. If the parameters $n = 1, k = 0, p = 0$, we can get Kerr black hole metric. In Ref. [72], Mazza et al. studied a special case of rotating black bounce space-time ($n = 1, k = 0$), and they further studied the quasinormal modes of this space-time [73].

In this work, we study the quasinormal modes of rotating black bounce spacetime for $n = 2, k = 0$. Therefore, the rotating black bounce space-time metric can be written as

$$ds^2 = - \left(1 - \frac{2M(r^2 + p^2)}{(r^4 + p^4)^{1/4} \Sigma} \right) dt^2 - \frac{4Ma(r^2 + p^2) \sin^2 \theta}{(r^4 + p^4)^{1/4} \Sigma} dt d\varphi + \frac{\Sigma}{\Delta} dr^2 + \Sigma d\theta^2 + \frac{A \sin^2 \theta}{\Sigma} d\varphi^2, \quad (5)$$

where

$$\begin{aligned} \Delta &= r^2 + a^2 + p^2 - \frac{2M(r^2 + p^2)}{(r^4 + p^4)^{1/4}}, \\ \Sigma &= r^2 + p^2 + a^2 \cos^2 \theta, \\ A &= [r^2 + a^2 + p^2]^2 - \Delta a^2 \sin^2 \theta. \end{aligned} \quad (6)$$

When the black hole spin $a = 0$, the rotating black bounce spacetime can degenerate to the black bounce spacetime studied in Ref. [79]. Moreover, this rotating black bounce space-time contains rotating black hole space-time and rotating wormhole space-time.

According to Kerr-like black bounce space-time metric (5), we can write its metric tensor

$$g_{\mu\nu} = \begin{pmatrix} - \left(1 - \frac{2M(r^2 + p^2)}{(r^4 + p^4)^{1/4} \Sigma} \right) & 0 & 0 & - \frac{2Ma(r^2 + p^2) \sin^2 \theta}{(r^4 + p^4)^{1/4} \Sigma} \\ 0 & \frac{\Sigma}{\Delta} & 0 & 0 \\ 0 & 0 & \Sigma & 0 \\ - \frac{2Ma(r^2 + p^2) \sin^2 \theta}{(r^4 + p^4)^{1/4} \Sigma} & 0 & 0 & \frac{A \sin^2 \theta}{\Sigma} \end{pmatrix}, \quad (7)$$

from which we can obtain the determinant of metric tensor

$$g \equiv \det(g_{\mu\nu}) = -\Sigma^2 \sin^2 \theta. \quad (8)$$

Therefore, the contravariant form of metric tensor $g^{\mu\nu}$ can be written as

$$g^{\mu\nu} = \begin{pmatrix} - \frac{A}{\Sigma \Delta} & 0 & 0 & - \frac{2Ma(r^2 + p^2)}{(r^4 + p^4)^{1/4} \Sigma \Delta} \\ 0 & \frac{\Delta}{\Sigma} & 0 & 0 \\ 0 & 0 & \frac{1}{\Sigma} & 0 \\ - \frac{2Ma(r^2 + p^2)}{(r^4 + p^4)^{1/4} \Sigma \Delta} & 0 & 0 & \frac{\Delta - a^2 \sin^2 \theta}{\Sigma \Delta \sin^2 \theta} \end{pmatrix}. \quad (9)$$

III. SCALAR PERTURBATION OF THE KERR-LIKE BLACK-BOUNCE SPACE-TIME

In this section, we will study the scalar perturbation of Kerr-like black-bounce space-time, and derive the effective potential of scalar particles in Kerr-like black-bounce space-time. To achieve this goal, we study Klein-Gordon equation. In curved spacetime, the Klein-Gordon equation can be written as

$$\frac{1}{\sqrt{-g}} \partial_\mu (\sqrt{-g} g^{\mu\nu} \partial_\nu \Psi) = \mu^2 \Psi, \quad (10)$$

with μ being the mass of the scalar particle. By bringing determinant of metric tensor (8) and the contravariant form of metric tensor $g^{\mu\nu}$ (9) into Klein-Gordon equation (10), we can write Eq. (10) as

$$-\frac{A}{\Sigma\Delta}\partial_t^2\Psi - \frac{2Ma(r^2+p^2)}{(r^4+p^4)^{1/4}\Sigma\Delta}\partial_t\partial_\phi\Psi + \frac{1}{\Sigma\sin\theta}\partial_\theta(\sin\theta\partial_\theta)\Psi + \frac{1}{\Sigma}\partial_r(\Delta\partial_r) - \frac{2Ma(r^2+p^2)}{(r^4+p^4)^{1/4}\Sigma\Delta}\partial_\phi\partial_t\Psi + \frac{\Delta - a^2\sin^2\theta}{\Delta\Sigma\sin^2\theta}\partial_\phi^2\Psi = \mu^2\Psi. \quad (11)$$

To carry out separation of variables, we can adopt the following ansatz

$$\Psi(r, t) = R_{lm}(r)S(\theta)e^{im\phi}e^{-i\omega t}, \quad (12)$$

with m being the azimuthal quantum number, and ω being the energy of the particles. Substituting it into Eq. (11), we can get the following second order partial differential radial equation

$$\frac{d}{dr}\left(\Delta\frac{dR_{lm}(r)}{dr}\right) + \left[\frac{\omega^2(r^2+a^2+p^2)^2 + m^2a^2}{\Delta} - (\omega^2a^2 + \mu^2(r^2+p^2)) - \frac{4Mam\omega(r^2+p^2)}{(r^4+p^4)^{1/4}\Delta}\right]R_{lm}(r) = 0, \quad (13)$$

and the angular equation can be read as

$$\frac{1}{\sin\theta}\frac{d}{d\theta}\left(\sin\theta\frac{dS_{lm}}{d\theta}\right) + \left[a^2(\omega^2 - \mu^2)\cos^2\theta - \frac{m^2}{\sin^2\theta}\right]S_{lm}(\theta) = 0. \quad (14)$$

The radial equation and the angular equation usually have the same eigenvalue Λ_{lm} , but the sign is opposite. These two equations can be solved by the separation constant method, so we consider the separation constant as eigenvalue Λ_{lm} . Then the second order partial differential radial equation becomes

$$\Delta\frac{d}{dr}\left(\Delta\frac{dR_{lm}(r)}{dr}\right) + \left\{m^2a^2 - \frac{4Mam\omega(r^2+p^2)}{(r^4+p^4)^{1/4}} + \omega^2(r^2+a^2+p^2)^2 - [\mu^2(r^2+p^2) + \omega^2a^2 + \Lambda_{lm}]\Delta\right\}R_{lm}(r) = 0. \quad (15)$$

The radial solution is usually related to the free oscillation mode of the propagating field, which has a specific frequency and its imaginary part is negative. In order to further derive the effective potential, we use the following transformation

$$R_{lm}(r) = \frac{\psi(r)}{\sqrt{r^2+a^2+p^2}}, \quad (16)$$

and tortoise coordinate

$$dr_* = \frac{r^2+a^2+p^2}{\Delta}dr. \quad (17)$$

Therefore, we obtain the following second-order partial differential equation about tortoise coordinates

$$\frac{d^2\psi}{dr_*^2} + (\omega^2 - V_{eff})\psi = 0, \quad (18)$$

where V_{eff} is the effective potential, which can be written as

$$V_{eff} = \frac{\Delta}{(a^2+r^2+p^2)^2}\left[\frac{r\Delta' + \Delta}{a^2+r^2+p^2} - \frac{3r^2\Delta}{(a^2+r^2+p^2)^2} - \frac{m^2a^2}{\Delta} + \frac{4Mam\omega(r^2+p^2)}{(r^4+p^4)^{1/4}\Delta} + \mu^2(r^2+p^2) + \omega^2a^2 + \Lambda_{lm}\right], \quad (19)$$

where Δ' represents the derivative $\frac{d\Delta}{dr}$. In Figs.1-3, we give the behavior of effective potential for different parameters. In Fig.1, the effective potential V_{eff} under the Kerr-like black bounce space-time scalar perturbation for different a is given. We can see that there are two peaks in effective potential, which is similar to effective potential of Schwarzschild-like black bounce space-time [79]. In Fig.2, we present the effective potential V_{eff} under the Kerr-like black bounce space-time scalar perturbation for different Λ_{lm} . It shown that effective potential is very sensitive to Λ_{lm} . Moreover, just focusing on the shape of effective potential, one can find that it is completely different from some other rotating black holes caused by modified gravity. In Fig.3, the effective potential V_{eff} under the Kerr-like black bounce space-time scalar perturbation for different p is presented.

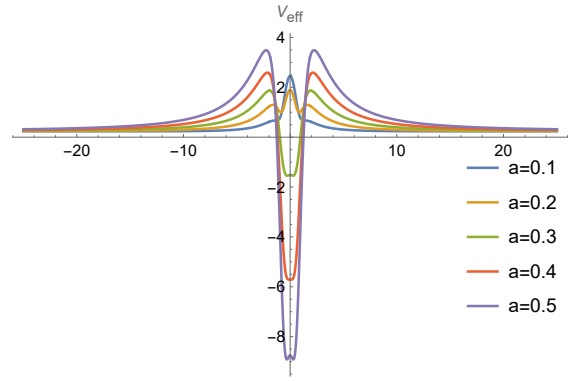


FIG. 1. Effective potential V_{eff} under the Kerr-like black bounce space-time scalar perturbation for different a with $p = 1, m = 1, M = 1, \mu = 0.5, \Lambda_{lm} = 2$.

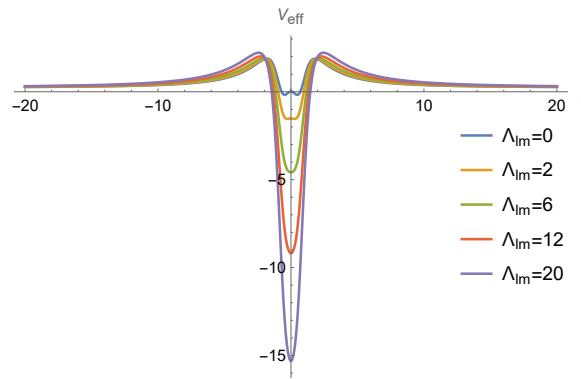


FIG. 2. Effective potential V_{eff} under the Kerr-like black bounce space-time scalar perturbation for different Λ_{lm} with $a = 0.3, p = 1, m = 1, M = 1, \mu = 0.5$.

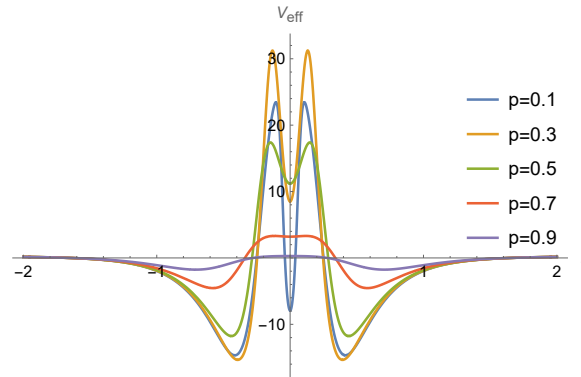


FIG. 3. Effective potential V_{eff} under the Kerr-like black bounce space-time scalar perturbation for different p with $a = 0.3, m = 1, M = 1, \mu = 0.5, \Lambda_{lm} = 2$.

IV. QNM OF THE KERR-LIKE BLACK BOUNCE SPACE-TIME

In this section, we briefly introduce Pöschl-Teller potential approximation and semi-analytic WKB method for calculating quasinormal modes of the Kerr-like black bounce space-time. We first introduce the relatively simple Pöschl-Teller potential approximation, which was suggested by B. Mashhoon [80, 81]. This method is mainly realized

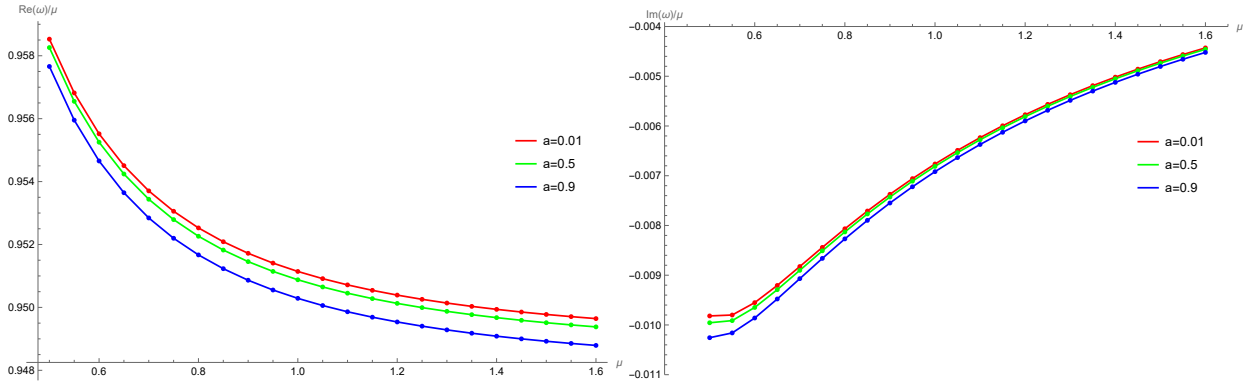


FIG. 4. Frequency spectrum of scalar perturbation of rotating black bounce space-time for different a with $m = 1, M = 1, p = 1, \Lambda_{lm} = 2$. The top panel is the oscillation frequency $\text{Re}\omega/\mu$, and bottom panel is the damping rate $\text{Im}\omega/\mu$, as the function of mass μ .

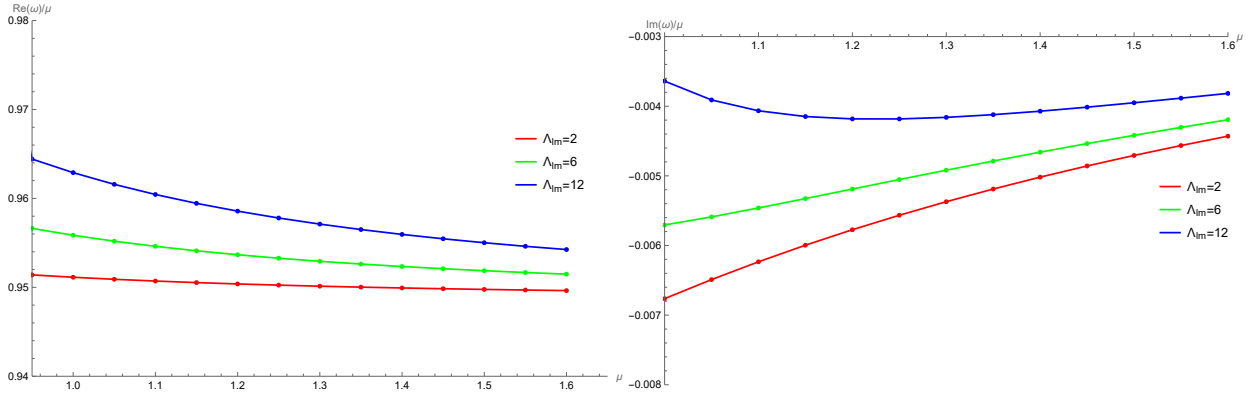


FIG. 5. Frequency spectrum of scalar perturbation of rotating black bounce space-time for different Λ_{lm} with $a = 0.1, m = 1, M = 1, p = 0.5$. The top panel is the oscillation frequency $\text{Re}\omega/\mu$, and bottom panel is the damping rate $\text{Im}\omega/\mu$, as the function of mass μ .

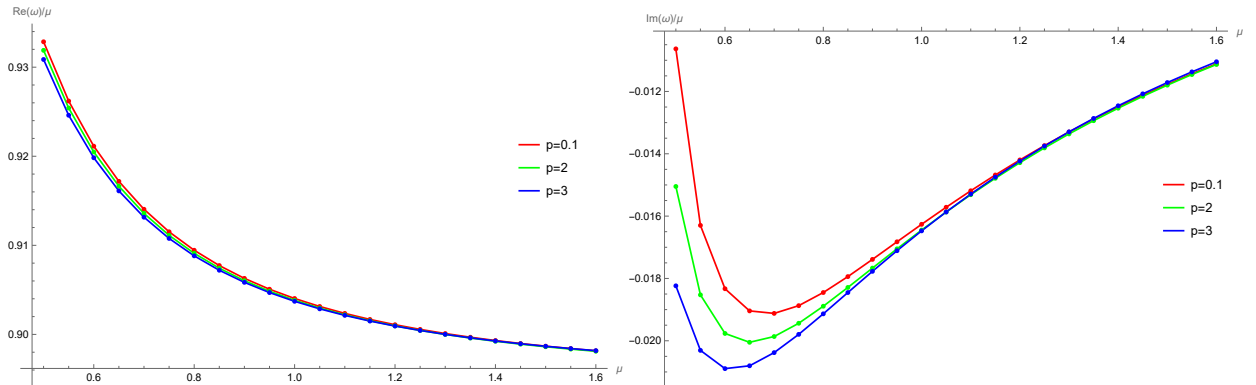


FIG. 6. Frequency spectrum of scalar perturbation of rotating black bounce space-time for different p with $a = 0.1, m = 1, M = 1, \Lambda_{lm} = 2$. The top panel is the oscillation frequency $\text{Re}\omega/\mu$, and bottom panel is the damping rate $\text{Im}\omega/\mu$, as the function of mass μ .

by approximating the effective potential, i.e. Pöschl-Teller potential, and its usual form is

$$V_{PT}(r_*) = \frac{V_0}{\cosh^2\left(\frac{r_*}{b}\right)}, \quad (20)$$

where

$$b = \frac{1}{\sqrt{-\frac{1}{2V_0} \frac{d^2V(r_{0*})}{dr_*^2}}}, \quad (21)$$

r_{0*} represents the position of the maximum value $V(r_*)$. We use V_0 to denote the maximum value of the effective potential. The basic computational idea is that map Eq. (18) to a Schrödinger-like wave equation, so that the solution of equation (18) satisfying the boundary condition

$$\begin{aligned} R(r_*) &\propto e^{i\omega r_*}, \text{ for } r_* \rightarrow \infty, \\ R(r_*) &\propto e^{-i\omega r_*}, \text{ for } r_* \rightarrow -\infty. \end{aligned} \quad (22)$$

Then, Eq. (18) can be mapped to the bound state of the new equation. One can analytically compute the bound states of the Schrödinger equation, so after obtaining them, we can obtain the QNM by considering the inverse mapping. To achieve this, the following transformations need to be considered

$$\begin{aligned} r_* &\rightarrow -ir_*, \\ (V_0, b) &\rightarrow (V_0, -ib). \end{aligned} \quad (23)$$

To remove the complexity of the expression, we let $p = (V_0, b)$ and $p' = (V_0, -ib)$, therefore we have

$$V(-ir_*, p') = V(r_*, p). \quad (24)$$

Moreover, by the definition

$$\begin{aligned} \phi(r_*, p) &= \psi(-ir_*, p'), \\ \Omega(p) &= \omega(p'), \end{aligned} \quad (25)$$

ϕ satisfies the equation

$$\frac{d^2\phi}{dr_*^2} + (-\Omega^2 + V)\phi = 0, \quad (26)$$

where

$$\Omega_n(V_0, b) = \frac{1}{b} \left[-\sqrt{\frac{1}{4} + V_0 b^2} + \left(n + \frac{1}{2}\right) \right]. \quad (27)$$

Therefore, we can get the QNM

$$\omega_n(V_0, b) = \Omega_n(V_0, ib) = \frac{1}{b} \left[\pm \sqrt{V_0 b^2 - \frac{1}{4}} - \left(n + \frac{1}{2}\right) i \right] \quad (28)$$

with the n being the integer $n \geq 0$.

On the other hand, in order to verify the accuracy of the results of the Pöschl-Teller potential approximation, we also use the WKB method [44, 82]. In the third order WKB method, we can obtain the QNM frequencies from the following equation

$$\omega^2 = \left[V_0 + \sqrt{-2V_0''} \Lambda(n) - i \left(n + \frac{1}{2}\right) \sqrt{-2V_0''} (1 + \Omega(n)) \right], \quad (29)$$

where

$$\Lambda(n) = \frac{1}{\sqrt{-2V_0}} \left[\frac{1}{8} \left(\frac{V_0^{(4)}}{V_0'} \right) \left(\frac{1}{4} + \alpha^2 \right) - \frac{1}{288} \left(\frac{V_0'}{V_0} \right)^2 (7 + 60\alpha^2) \right], \quad (30)$$

with

$$\Omega(n) = \frac{1}{-2V_0'} \left[\frac{5}{6912} \left(\frac{V_0'}{V_0} \right)^4 (77 + 188\alpha^2) - \frac{1}{384} \left(\frac{V_0'^2 V_0^{(4)}}{V_0^3} \right) (51 + 100\alpha^2) + \right. \\ \left. \frac{1}{2304} \left(\frac{V_0^{(4)}}{V_0'} \right)^2 (67 + 68\alpha^2) + \frac{1}{288} \left(\frac{V_0' V_0^{(5)}}{V_0^2} \right) (19 + 28\alpha^2) - \frac{1}{288} \left(\frac{V_0^{(6)}}{V_0'} \right) (5 + 4\alpha^2) \right], \quad (31)$$

where prime represents the derivation respect to r_* , and $\alpha = n + \frac{1}{2}$. $V_0^{(n)}$ denotes the n -order derivative of the effective potential. Moreover, sixth order WKB method is given by

$$\frac{i(\omega^2 - V_0)}{\sqrt{-2V_0''}} - \sum_{i=2}^6 \Lambda_i = n + \frac{1}{2}, \quad n = 0, 1, 2, \dots, \quad (32)$$

where the WKB corrections term Λ_i is given in Ref. [83], and V_0 denotes the maximum of effective potential. In TABLE I, we compare the QNM frequencies calculated by the above two methods, and one can find that the results of the Pöschl-Teller potential approximation are in good agreement with the results of the semi-analytic WKB method. Furthermore, the results show that with the increase of the spin parameter a , the actual oscillation frequencies and damping rate of the quasinormal modes in Kerr-like black bounce space-time will decrease, that is, they are inversely proportional to the spin parameter a . This demonstrates that when the Kerr-like black bounce space-time rotates faster, its decay rate is slower after perturbations. In Fig. 4, we show the actual oscillation frequencies and the damping rate of scalar perturbation of rotating black bounce space-time for different spin a with $m = 1, M = 1, p = 1, \Lambda_{lm} = 2$. In Fig. 5, the frequency spectrum of scalar perturbation of rotating black bounce space-time for different Λ_{lm} with $a = 0.1, m = 1, M = 1, p = 0.5$ are presented. In Fig. 6, we give the frequency spectrum of scalar perturbation of rotating black bounce space-time for different p with $a = 0.1, m = 1, M = 1, \Lambda_{lm} = 2$.

TABLE I. QNM frequencies of scalar field perturbation for $l = 1, m = 0, p = 1, \mu = 0$.

a	Pöschl-Teller	3th order WKB	6th order WKB
0.0	0.27997 - 0.096956i	0.271768 - 0.0937156i	0.274464 - 0.093496i
0.1	0.279558 - 0.0967096i	0.271429 - 0.0935124i	0.274117 - 0.0932881i
0.2	0.278329 - 0.0959766i	0.270418 - 0.0929065i	0.273079 - 0.0926693i
0.3	0.276305 - 0.0947754i	0.268743 - 0.0919089i	0.271359 - 0.0916531i
0.4	0.273517 - 0.0931353i	0.266422 - 0.0905372i	0.268974 - 0.0902618i
0.5	0.270009 - 0.0910954i	0.263478 - 0.0888155i	0.265947 - 0.0885243i
0.6	0.265836 - 0.0887018i	0.25994 - 0.0867728i	0.262307 - 0.0864758i
0.7	0.261057 - 0.0860059i	0.255842 - 0.0844428i	0.258091 - 0.0841548i
0.8	0.255737 - 0.0830621i	0.251223 - 0.0818623i	0.253341 - 0.0816021i
0.9	0.249943 - 0.0799257i	0.246125 - 0.0790703i	0.248105 - 0.078859i

V. SUMMARY AND OUTLOOK

In this work we have analyzed the quasinormal modes of a Kerr-like black-bounce spacetime sourced by massive scalar-field perturbations. Our primary goal was to understand how deviations from the Kerr geometry, encoded in the bounce parameter p and in the underlying black-bounce construction, modify the ringdown spectrum and potentially leave observable signatures in gravitational-wave signals.

Starting from the Kerr-like black-bounce metric obtained via the Newman–Janis algorithm [75], and specializing to the case $n = 2$ and $k = 0$, we derived the scalar-field Klein–Gordon equation in this background. By separating variables, we obtained the radial and angular equations and recast the radial sector into a Schrödinger-like form in terms of the tortoise coordinate. This allowed us to identify an effective potential $V_{\text{eff}}(r)$, whose structure we studied as a function of the spin parameter a , the bounce parameter p , the separation constant Λ_{lm} , and the scalar-field mass μ .

We showed that the Kerr-like black-bounce spacetime exhibits a characteristic double-peaked effective potential, closely analogous to the Schwarzschild-like black-bounce case [79] and qualitatively different from the effective potentials of many other Kerr-like black holes in modified gravity theories [84] or in dark-matter halos [85]. This double-barrier structure is known to be closely related to the appearance of gravitational-wave echoes at late times, and therefore makes the rotating black-bounce geometry a promising candidate for echo searches.

To compute the QNM spectrum, we employed two complementary semi-analytic methods: the Pöschl–Teller potential approximation and the WKB approach (up to sixth order). We verified that, for the parameter ranges considered, the QNM frequencies obtained from these methods are in good agreement, as summarized in Table I. We then systematically explored the dependence of the real and imaginary parts of the frequencies on the spin a , the bounce parameter p , the separation constant Λ_{lm} , and the scalar mass μ , presenting our results in Figs. 4–6.

Our main physical findings can be summarized as follows:

- For fixed μ and p , increasing the spin parameter a reduces both the real part of the frequency and the magnitude of the imaginary part. In other words, as the Kerr-like black-bounce object spins faster, the oscillation frequency of the scalar QNMs decreases and the modes become longer-lived (the damping rate decreases in magnitude).
- The bounce parameter p , which controls whether the geometry corresponds to a black hole or a wormhole and encodes the deviation from the Kerr solution, has a qualitatively similar effect: larger p lowers the QNM frequencies and suppresses the damping rate. This implies that more strongly “bounced” or wormhole-like configurations exhibit slower decay of perturbations.
- The mass μ of the scalar field significantly affects the QNM spectrum: massive modes develop a richer structure in the (μ, ω) plane and contribute to shifting both the real and imaginary parts of the frequencies. Thus, even at the level of test fields, the mass term should not be neglected when modeling ringdowns in such backgrounds.

Taken together, these results indicate that Kerr-like black-bounce spacetimes can mimic Kerr black holes at the level of global properties while still leaving distinct imprints in the detailed time-domain response to perturbations, particularly through modified QNM spectra and the possibility of echo-like features associated with double-peaked effective potentials [65, 79]. From the observational perspective, current and future gravitational-wave detectors — including the LIGO/Virgo/KAGRA network and the planned space-based mission LISA [10] — offer an exciting opportunity to search for such signatures and to constrain deviations from the Kerr paradigm.

Several natural extensions of this work suggest themselves. One important next step is a full time-domain analysis of scalar (and gravitational) perturbations in Kerr-like black-bounce spacetimes, aimed specifically at resolving the echo structure and quantifying its dependence on (a, p) and on the type of perturbation. Another direction is to move beyond test fields and study axial and polar gravitational perturbations, possibly within a gauge-invariant formalism, in order to connect more directly with the gravitational-wave polarizations measured by detectors. It would also be interesting to investigate superradiant scattering and possible instability windows for massive fields in the Kerr-like black-bounce background, as well as to explore the impact of dark-matter environments and plasma effects on the QNM spectrum.

We hope that the present analysis provides a useful step toward a systematic characterization of rotating black-bounce spacetimes as potential black-hole mimickers, and toward leveraging ringdown and echo observations as precision probes of regular cores, wormhole-like interiors, and more general deviations from the Kerr geometry.

ACKNOWLEDGMENTS

We are very grateful for Prof. A. Zhidenko useful correspondence. This research was funded by the National Natural Science Foundation of China (No. 12505064), Guizhou Provincial Basic Research Program (Natural Science) Youth Guidance Program (No. QN [2025] 365), the project of Young Scientific and Technical Talents Development of Education Department of Guizhou Province under Grant [2024] 79 and the Science and Technology Foundation of Guizhou Province (No.ZK[2022]YB029). A. Ö. would like to acknowledge networking support of the COST Action CA21106 - COSMIC WISPerS in the Dark Universe: Theory, astrophysics and experiments (CosmicWISPerS), the COST Action CA22113 - Fundamental challenges in theoretical physics (THEORY-CHALLENGES), the COST Action CA21136 - Addressing observational tensions in cosmology with systematics and fundamental physics (CosmoVerse), the COST Action CA23130 - Bridging high and low energies in search of quantum gravity (BridgeQG), and the COST Action CA23115 - Relativistic Quantum Information (RQI) funded by COST (European Cooperation in Science and Technology). A. Ö. also thanks to EMU, TUBITAK, ULAKBIM (Turkiye) and SCOAP3 (Switzerland)

for their support.

-
- [1] B. P. Abbott *et al.* (LIGO Scientific, Virgo), *Phys. Rev. Lett.* **116**, 061102 (2016), arXiv:1602.03837 [gr-qc].
- [2] K. Akiyama *et al.* (Event Horizon Telescope), *Astrophys. J. Lett.* **875**, L1 (2019), arXiv:1906.11238 [astro-ph.GA].
- [3] K. Akiyama *et al.*, *Astrophys. J. Lett.* **930**, L12 (2022).
- [4] L. Barack *et al.*, *Class. Quant. Grav.* **36**, 143001 (2019), arXiv:1806.05195 [gr-qc].
- [5] M. Martinelli and S. Casas, *Universe* **7**, 506 (2021), arXiv:2112.10675 [astro-ph.CO].
- [6] C.-Y. Chen, M. Bouhmadi-López, and P. Chen, *Eur. Phys. J. Plus* **136**, 253 (2021), arXiv:2103.01249 [gr-qc].
- [7] E. Berti *et al.*, *Class. Quant. Grav.* **32**, 243001 (2015), arXiv:1501.07274 [gr-qc].
- [8] I. Çimdiker, D. Demir, and A. Övgün, *Phys. Dark Univ.* **34**, 100900 (2021), arXiv:2110.11904 [gr-qc].
- [9] V. Cardoso, E. Franzin, and P. Pani, *Phys. Rev. Lett.* **116**, 171101 (2016), [Erratum: *Phys.Rev.Lett.* **117**, 089902 (2016)], arXiv:1602.07309 [gr-qc].
- [10] E. Barausse *et al.*, *Gen. Rel. Grav.* **52**, 81 (2020), arXiv:2001.09793 [gr-qc].
- [11] W.-L. Qian, K. Lin, X.-M. Kuang, B. Wang, and R.-H. Yue, *Eur. Phys. J. C* **82**, 188 (2022), arXiv:2109.02844 [gr-qc].
- [12] X.-M. Kuang and J.-P. Wu, *Phys. Lett. B* **770**, 117 (2017), arXiv:1702.01490 [hep-th].
- [13] S. Fernando, *Gen. Rel. Grav.* **48**, 24 (2016), arXiv:1601.06407 [gr-qc].
- [14] S. Fernando and J. Correa, *Phys. Rev. D* **86**, 064039 (2012), arXiv:1208.5442 [gr-qc].
- [15] S. Fernando, *Gen. Rel. Grav.* **36**, 71 (2004), arXiv:hep-th/0306214.
- [16] S. Fernando, *Phys. Rev. D* **79**, 124026 (2009), arXiv:0903.0088 [hep-th].
- [17] S. Fernando, *Phys. Rev. D* **77**, 124005 (2008), arXiv:0802.3321 [hep-th].
- [18] S. Fernando and T. Clark, *Gen. Rel. Grav.* **46**, 1834 (2014), arXiv:1411.6537 [gr-qc].
- [19] V. Cardoso, S. Hopper, C. F. B. Macedo, C. Palenzuela, and P. Pani, *Phys. Rev. D* **94**, 084031 (2016), arXiv:1608.08637 [gr-qc].
- [20] V. Cardoso and P. Pani, *Nature Astron.* **1**, 586 (2017), arXiv:1709.01525 [gr-qc].
- [21] E. Maggio, A. Testa, S. Bhagwat, and P. Pani, *Phys. Rev. D* **100**, 064056 (2019), arXiv:1907.03091 [gr-qc].
- [22] R. A. Konoplya and A. Zhidenko, (2022), arXiv:2203.16635 [gr-qc].
- [23] R. A. Konoplya, Z. Stuchlík, and A. Zhidenko, *Phys. Rev. D* **99**, 024007 (2019), arXiv:1810.01295 [gr-qc].
- [24] K. A. Bronnikov and R. A. Konoplya, *Phys. Rev. D* **101**, 064004 (2020), arXiv:1912.05315 [gr-qc].
- [25] M. S. Churilova, R. A. Konoplya, Z. Stuchlík, and A. Zhidenko, *JCAP* **10**, 010 (2021), arXiv:2107.05977 [gr-qc].
- [26] A. Simpson and M. Visser, *Phys. Rev. D* **105**, 064065 (2022), arXiv:2112.04647 [gr-qc].
- [27] A. Simpson and M. Visser, *JCAP* **03**, 011 (2022), arXiv:2111.12329 [gr-qc].
- [28] S. Shankaranarayanan and J. P. Johnson, *Gen. Rel. Grav.* **54**, 44 (2022), arXiv:2204.06533 [gr-qc].
- [29] S. D. Odintsov, V. K. Oikonomou, and R. Myrzakulov, *Symmetry* **14**, 729 (2022), arXiv:2204.00876 [gr-qc].
- [30] T. Baker *et al.*, *Rev. Mod. Phys.* **93**, 015003 (2021), arXiv:1908.03430 [astro-ph.CO].
- [31] P. G. Ferreira, *Ann. Rev. Astron. Astrophys.* **57**, 335 (2019), arXiv:1902.10503 [astro-ph.CO].
- [32] R. C. Pantig and A. Övgün, *Eur. Phys. J. C* **82**, 391 (2022), arXiv:2201.03365 [gr-qc].
- [33] R. C. Pantig, P. K. Yu, E. T. Rodulfo, and A. Övgün, *Annals of Physics* **436**, 168722 (2022).
- [34] D. Kubiznak and R. B. Mann, *JHEP* **07**, 033 (2012), arXiv:1205.0559 [hep-th].
- [35] S. Gunasekaran, R. B. Mann, and D. Kubiznak, *JHEP* **11**, 110 (2012), arXiv:1208.6251 [hep-th].
- [36] R. Kerner and R. B. Mann, *Phys. Lett. B* **665**, 277 (2008), arXiv:0803.2246 [hep-th].
- [37] E. T. Akhmedov, V. Akhmedova, and D. Singleton, *Phys. Lett. B* **642**, 124 (2006), arXiv:hep-th/0608098.
- [38] D. Singleton and S. Wilburn, *Phys. Rev. Lett.* **107**, 081102 (2011), arXiv:1102.5564 [gr-qc].
- [39] R. G. Daghigh and M. D. Green, *Class. Quant. Grav.* **26**, 125017 (2009), arXiv:0808.1596 [gr-qc].
- [40] R. G. Daghigh and M. D. Green, *Phys. Rev. D* **85**, 127501 (2012), arXiv:1112.5397 [gr-qc].
- [41] R. G. Daghigh, M. D. Green, J. C. Morey, and G. Kunstatter, *Phys. Rev. D* **102**, 104040 (2020), arXiv:2009.02367 [gr-qc].
- [42] A. Zhidenko, *Class. Quant. Grav.* **21**, 273 (2004), arXiv:gr-qc/0307012.
- [43] A. Zhidenko, *Class. Quant. Grav.* **23**, 3155 (2006), arXiv:gr-qc/0510039.
- [44] R. A. Konoplya and A. Zhidenko, *Rev. Mod. Phys.* **83**, 793 (2011), arXiv:1102.4014 [gr-qc].
- [45] M. Chabab, H. El Moumni, S. Iraoui, and K. Masmar, *Astrophys. Space Sci.* **362**, 192 (2017), arXiv:1701.00872 [hep-th].
- [46] S. Lepe and J. Saavedra, *Phys. Lett. B* **617**, 174 (2005), arXiv:gr-qc/04110074.
- [47] P. A. González, E. Papantonopoulos, J. Saavedra, and Y. Vásquez, *Phys. Rev. D* **95**, 064046 (2017), arXiv:1702.00439 [gr-qc].
- [48] M. Okyay and A. Övgün, *JCAP* **01**, 009 (2022), arXiv:2108.07766 [gr-qc].
- [49] P. A. González, A. Rincón, J. Saavedra, and Y. Vásquez, *Phys. Rev. D* **104**, 084047 (2021), arXiv:2107.08611 [gr-qc].
- [50] G. Panotopoulos and A. Rincón, *Phys. Dark Univ.* **31**, 100743 (2021), arXiv:2011.02860 [gr-qc].
- [51] G. Panotopoulos and A. Rincón, *Eur. Phys. J. Plus* **135**, 33 (2020), arXiv:1910.08538 [gr-qc].
- [52] G. Panotopoulos and A. Rincón, *Eur. Phys. J. Plus* **134**, 300 (2019), arXiv:1904.10847 [gr-qc].
- [53] A. Rincón and G. Panotopoulos, *Phys. Rev. D* **97**, 024027 (2018), arXiv:1801.03248 [hep-th].
- [54] A. Övgün and K. Jusufi, *Annals Phys.* **395**, 138 (2018), arXiv:1801.02555 [gr-qc].
- [55] E. Berti, V. Cardoso, and A. O. Starinets, *Class. Quant. Grav.* **26**, 163001 (2009), arXiv:0905.2975 [gr-qc].
- [56] V. Cardoso, A. S. Miranda, E. Berti, H. Witek, and V. T. Zanchin, *Phys. Rev. D* **79**, 064016 (2009), arXiv:0812.1806 [hep-th].
- [57] N. Andersson and C. J. Howls, *Class. Quant. Grav.* **21**, 1623 (2004), arXiv:gr-qc/0307020.

- [58] N. Andersson, *Phys. Rev. D* **55**, 468 (1997), [arXiv:gr-qc/9607064](#).
- [59] N. Andersson and H. Onozawa, *Phys. Rev. D* **54**, 7470 (1996), [arXiv:gr-qc/9607054](#).
- [60] N. Andersson and S. Linnæus, *Phys. Rev. D* **46**, 4179 (1992).
- [61] N. Andersson, *Phys. Rev. D* **51**, 353 (1995).
- [62] B. Wang, E. Abdalla, and R. B. Mann, *Phys. Rev. D* **65**, 084006 (2002), [arXiv:hep-th/0107243](#).
- [63] A. Simpson and M. Visser, *JCAP* **02**, 042 (2019), [arXiv:1812.07114 \[gr-qc\]](#).
- [64] F. S. N. Lobo, M. E. Rodrigues, M. V. d. S. Silva, A. Simpson, and M. Visser, *Phys. Rev. D* **103**, 084052 (2021), [arXiv:2009.12057 \[gr-qc\]](#).
- [65] M. S. Churilova and Z. Stuchlik, *Class. Quant. Grav.* **37**, 075014 (2020), [arXiv:1911.11823 \[gr-qc\]](#).
- [66] K. A. Bronnikov, R. A. Konoplya, and T. D. Pappas, *Phys. Rev. D* **103**, 124062 (2021), [arXiv:2102.10679 \[gr-qc\]](#).
- [67] J. R. Nascimento, A. Y. Petrov, P. J. Porfírio, and A. R. Soares, *Phys. Rev. D* **102**, 044021 (2020), [arXiv:2005.13096 \[gr-qc\]](#).
- [68] N. Tsukamoto, *Phys. Rev. D* **103**, 024033 (2021), [arXiv:2011.03932 \[gr-qc\]](#).
- [69] A. Övgün, *Turk. J. Phys.* **44**, 465 (2020), [arXiv:2011.04423 \[gr-qc\]](#).
- [70] H. C. D. Lima, C. L. Benone, and L. C. B. Crispino, *Phys. Rev. D* **101**, 124009 (2020), [arXiv:2006.03967 \[gr-qc\]](#).
- [71] F. S. N. Lobo, A. Simpson, and M. Visser, *Phys. Rev. D* **101**, 124035 (2020), [arXiv:2003.09419 \[gr-qc\]](#).
- [72] J. Mazza, E. Franzin, and S. Liberati, *JCAP* **04**, 082 (2021), [arXiv:2102.01105 \[gr-qc\]](#).
- [73] E. Franzin, S. Liberati, J. Mazza, R. Dey, and S. Chakraborty, (2022), [arXiv:2201.01650 \[gr-qc\]](#).
- [74] E. Franzin, S. Liberati, J. Mazza, A. Simpson, and M. Visser, *JCAP* **07**, 036 (2021), [arXiv:2104.11376 \[gr-qc\]](#).
- [75] Z. Xu and M. Tang, *Eur. Phys. J. C* **81**, 863 (2021), [arXiv:2109.13813 \[gr-qc\]](#).
- [76] M. Guerrero, G. J. Olmo, D. Rubiera-Garcia, and D. S.-C. Gómez, *JCAP* **08**, 036 (2021), [arXiv:2105.15073 \[gr-qc\]](#).
- [77] M.-Y. Ou, M.-Y. Lai, and H. Huang, (2021), [arXiv:2111.13890 \[gr-qc\]](#).
- [78] N. Tsukamoto, *Phys. Rev. D* **105**, 084036 (2022), [arXiv:2202.09641 \[gr-qc\]](#).
- [79] Y. Yang, D. Liu, Z. Xu, Y. Xing, S. Wu, and Z.-W. Long, *Phys. Rev. D* **104**, 104021 (2021), [arXiv:2107.06554 \[gr-qc\]](#).
- [80] H.-J. Blome and B. Mashhoon, *Physics Letters A* **100**, 231 (1984).
- [81] V. Ferrari and B. Mashhoon, *Phys. Rev. D* **30**, 295 (1984).
- [82] R. A. Konoplya, A. Zhidenko, and A. F. Zinhailo, *Class. Quant. Grav.* **36**, 155002 (2019), [arXiv:1904.10333 \[gr-qc\]](#).
- [83] S. Iyer and C. M. Will, *Phys. Rev. D* **35**, 3621 (1987).
- [84] M. Sharif and Q. Ama-Tul-Mughani, *PTEP* **2020**, 033E01 (2020).
- [85] D. Liu, Y. Yang, A. Övgün, Z.-W. Long, and Z. Xu, *Eur. Phys. J. C* **83**, 565 (2023), [arXiv:2204.11563 \[gr-qc\]](#).